AMERICAN ACADEMY OF OPHTHALMOLOGY®

Quantitative Evaluation of Choroidal Neovascularization under Pro Re Nata Anti–Vascular Endothelial Growth Factor Therapy with OCT Angiography

Scott M. McClintic, MD, Simon Gao, PhD, Jie Wang, MS, Ahmed Hagag, MD, Andreas K. Lauer, MD, Christina J. Flaxel, MD, Kavita Bhavsar, MD, Thomas S. Hwang, MD, David Huang, MD, PhD, Yali Jia, PhD, Steven T. Bailey, MD

Purpose: To use OCT angiography (OCTA)-derived quantitative metrics to assess the response of choroidal neovascularization (CNV) to pro re nata (PRN) anti–vascular endothelial growth factor (VEGF) treatment in neovascular age-related macular degeneration (AMD).

Design: Prospective, longitudinal cohort study.

Participants: Fourteen eyes from 14 study participants with treatment-naïve neovascular AMD were enrolled.

Methods: Participants were evaluated monthly and treated with intravitreal anti-VEGF agents under a PRN protocol for 1 year. At each visit, two 3 × 3-mm^2 OCTA scans were obtained. Custom image processing was applied to segment the outer retinal slab, suppress projection artifact, and automatically detect CNV. Choroidal neovascularization membrane area and CNV vessel area were calculated.

Main Outcome Measures: Individual and mean CNV membrane area and CNV vessel area at each visit; within-visit repeatability determined by coefficient of variation.

Results: Eight eyes showed the entire CNV to be within the 3 × 3-mm^2 scanning area and had adequate image quality for CNV quantification. One patient (patient 2) was excluded from analysis because of the presence of a large subretinal hemorrhage overlying the CNV membrane. In the remaining patients, CNV vessel area was reduced by 39%, 50%, 43%, and 41% at months 1, 3, 6, and 12, respectively. Choroidal neovascularization membrane area was reduced by 39%, 51%, 54%, and 45% at months 1, 3, 6, and 12. At month 6, mean change from baseline was not statistically significant for CNV vessel area, whereas it was statistically significant for CNV membrane area. Neither metric was significantly different compared with baseline at month 12. Individual analyses revealed each CNV had a unique response under PRN treatment. Within-visit repeatability was 7.96% (coefficient of variation) for CNV vessel area and 7.37% for CNV membrane area.

Conclusions: In this small exploratory study of CNV response to PRN anti-VEGF treatment, both CNV vessel area and membrane area were reduced compared with baseline after 3 months. After 1 year of follow-up, these reductions were no longer statistically significant. When anti-VEGF treatment was withheld, increasing CNV vessel area over time often resulted in exudation, but it was not possible to determine exactly when exudation occurs. *Ophthalmology Retina 2018;■:1–11 © 2018 by the American Academy of Ophthalmology*

Age-related macular degeneration (AMD) is a leading cause of vision loss. Neovascular AMD accounts for most vision loss and is characterized by the formation of choroidal neovascularization (CNV).[1] Although fluorescein angiography (FA) is the gold standard for CNV diagnosis,[2] structural OCT is helpful for CNV diagnosis and is an indispensable tool for monitoring response to treatment.[3]

Treatment of neovascular AMD with anti–vascular endothelial growth factor (VEGF) intravitreal injections given monthly is highly effective in preventing vision loss and improving vision in approximately 30% of patients over the course of 2 years.[4] However, if anti-VEGF therapy is switched to quartile dosing after 3 fixed monthly loading treatments, visual acuity benefit is not as robust as with fixed monthly dosing.[5,6] Several studies have shown that by using structural OCT to guide anti-VEGF treatment decisions, pro re nata (PRN) and treat-and-extend strategies can maintain the visual acuity benefits of monthly anti-VEGF treatment while reducing the number of injections needed.[7,8] A limitation of structural OCT is that it detects exudation associated with CNV, but cannot easily be used to evaluate changes in CNV size, morphologic structure, or CNV blood flow. Choroidal neovascularization area can be calculated with FA and indocyanine green angiography (ICGA), and changes in CNV area in response to anti-VEGF treatment

https://doi.org/10.1016/j.oret.2018.01.014
ISSN 2468-6530/18

have been demonstrated using these methods.[4,9] However, dye-based angiography is invasive and time consuming, and it is not used routinely to help make treatment decisions.

OCT angiography (OCTA) is a new technology that detects moving red blood cells as variations in OCT amplitude, phase, or complex signals over time from B-scans acquired at the same position.[10,11] Intravenous contrast agents are not required, and scans are acquired quickly at the rate of approximately 4 seconds per scan. These features are desirable for both patient safety and clinic workflow. The 3-dimensional images produced by OCTA allow for visualization of individual retinal and choroidal circulations based on their relative depths, a feature not possible with traditional dye-based angiography.

Recent studies have demonstrated that OCTA is a useful technique for noninvasive CNV detection.[12–17] Choroidal neovascularization is identified as blood flow in the outer retinal slab, which is defined as the region between Bruch's membrane and the outer border of the outer plexiform layer.[13] In healthy eyes, this area is devoid of blood flow. With FA, detailed discrimination of CNV architecture is impaired by leakage of fluorescein and the blockage of fluorescence by the retinal pigment epithelium (RPE); in contrast, OCTA images of CNV are not obscured by leakage or dye blockage from the RPE, allowing for superior resolution of CNV vascular branches. Structural OCT is obtained simultaneously along with the OCT angiogram, and combining color-coded cross-sectional OCTA images with structural OCT images may illustrate novel structure and blood flow relationships. Choroidal neovascularization characterization with OCTA is analogous to histologic classification described by Gass, with type 1 CNV identified as flow beneath the RPE and type 2 as flow above the RPE in the subretinal space.[13,18]

Several studies have reported changes in CNV morphologic features and changes in CNV size in response to anti-VEGF treatment.[15,18–21] Using OCTA to develop reliable, repeatable, and quantifiable CNV metrics may facilitate clarification and practical evaluation of the relationship between changes in CNV morphologic features and treatment response. Before clinical implementation is possible, several challenges must be addressed. First, most techniques evaluating CNV size rely on manual contouring of the CNV lesion by the investigator, which may not be practical in a busy clinical setting. Second, automated OCT segmentation is prone to errors with retinal architecture irregularities such as those produced by intraretinal fluid (IRF), subretinal fluid (SRF), hyperreflective material, and pigment epithelial detachment. Third, projection artifacts may interfere with precise evaluation of neovascular vessels. This may occur when superficial vessel projection artifacts are included in the outer retinal slab. Fourth, measurement repeatability has not been evaluated sufficiently, making it difficult to determine whether observed differences represent true changes. Finally, it is not known which quantitative metrics would yield the most relevant clinical information and which would be best suited to guide anti-VEGF therapy.

We recently developed a semiautomated CNV quantification algorithm that has been applied to commercially available OCTA. This technique uses a semiautomated segmentation strategy to ensure that appropriate boundaries of the outer retinal–RPE slab are identified consistently, and a saliency-based algorithm for automatic CNV detection and quantification.[22,23] A prospective cohort of treatment-naïve study participants was followed up under a PRN treatment regimen to determine if OCTA provides novel information that clinicians may use to develop individualized treatment strategies.

Methods

This prospective, longitudinal study received approval by the institutional review board at Oregon Health and Science University. Consecutive patients with treatment-naïve neovascular AMD provided informed consent to be scanned with monthly spectral-domain (SD)-OCTA scans (Avanti XR; Optovue, Inc., Fremont, CA) while receiving PRN anti-VEGF treatment for 1 year. At the beginning of the study, OCTA had not yet obtained Food and Drug Administration approval. The goal of the study was to determine how OCTA quantitative features change during the first year of treatment with anti-VEGF therapy. Study participants were recruited from the retina clinics at the Casey Eye Institute (Oregon Health and Science University, Portland, OR) from September 2014 through December 2015. Visual acuity (using the Early Treatment Diabetic Retinopathy Study chart), slit-lamp examination, dilated fundus examination, structural SD-OCT (Spectralis; Heidelberg Engineering, Germany), FA, and OCTA were performed at baseline. Each of these evaluations, except for FA, was repeated at each subsequent follow-up visit.

Choroidal neovascularization type was classified as either classic, occult, minimally classic, or retinal angiomatous proliferation, based on interpretation of the FA image by 2 trained vitreoretinal surgeons (S.M.M. and S.T.B.). All study participants were treated at the initial visit with an intravitreal injection of an anti-VEGF agent in the study eye. Each participant was followed up monthly for 1 year. After initial treatment at baseline visit, subsequent anti-VEGF treatment was given on a PRN basis. Treatment was administered for any one of the following conditions: reduction in Early Treatment Diabetic Retinopathy Study visual acuity; the presence of associated subretinal hemorrhage (SRH) or intraretinal hemorrhage; and the presence of SRF, IRF, or sub-RPE fluid on SD-OCT. The protocol was similar to the Comparison of Age-Related Macular Degeneration Treatments Trials and did not require 3 initial consecutive monthly injections.[7]

OCT angiography was performed using the 70-kHz RTVue-XR Avanti SD-OCT system (Optovue, Inc.), which has a wavelength spectrum centered at 840 nm and a 5-μm full-width half-maximum resolution in tissue. Two 3 × 3-mm scans (304 × 304 × 2 A-scans) centered on the macula were obtained for each study eye at each visit. After the first scan, the participant was instructed to remove the chin from the chin rest and wait at least 30 seconds before the second scan was conducted. Angiograms were exported to the Casey Eye Reading Center for custom processing. A semiautomated segmentation algorithm separated the angiogram into an inner retinal slab, an outer retinal slab, and a choroidal slab. Accuracy of segmentation was reviewed by a grader (S.G.) and corrected manually if needed. Choroidal neovascularization was detected in the outer retinal slab, between the outer boundary of the outer plexiform layer and Bruch's membrane. Any en face inner retinal shadow graphic projection artifact was removed with a slab subtraction technique using a Gaussian-filtered version of the inner retinal angiogram, which then was subtracted from the outer retinal angiogram. A saliency-based method was used to detect CNV

Table 1. Choroidal Neovascularization Vessel Area in Response to Pro Re Nata Anti–Vascular Endothelial Growth Factor Treatment

Patient No.	Age (yrs)	Initial Visual Acuity	Lesion Type		Choroidal Neovascularization Vessel Area (mm^2)							
			Fluorescein Angiography	*OCT Angiography*	*Initial*	*After 1 Month*	*Change from Baseline (%)*	*After 3 Months*	*Change from Baseline (%)*	*After 6 Months*	*Change from Baseline (%)*	*After Approximately 12 Months*	*Change from Baseline (%)*
1	69	20/25	Occult	1	0.33	0.26	−21	0.21	−38	0.34	3	0.08	−75
2*	68	20/50	Occult	1	0.62	0.85	37	1.32	112	1.43	130	0.73	18
3	80	20/50	Occult	1	0.83	0.74	−12	0.75	−10	0.99	18	0.65	−22
4*	65	20/20	Occult	1	0.19	0.14	−23	0.14	−27	0.12	−36	0.14	−27
5	77	20/20	Occult	1	0.52	0.50	−4	0.33	−37	0.31	−40	0.70	35
6	57	20/80	Classic	2	0.65	0.32	−51	0.40	−38	0.29	−55	0.38	−41
7	66	20/50	Classic	2	0.17	0.07	−60	0	−100	0.01	−92	0.07	−57
8	76	20/80+6	RAP	3	0.02	0	−100	0	−100	0	−100	0	−100
Average†					0.39±0.29	0.29±0.26‡	−39±34	0.26±0.26‡	−50±36	0.29±0.34	−43±44	0.29±0.29	−41±43

RAP = retinal angiomatous proliferation.
*Indicates participant was treated at every visit.
†Average (mean ± standard deviation) values do not include patient 2.
‡$P < 0.05$ when compared with baseline (Wilcoxon test); does not include patient 2.

automatically.[22] Only cases in which the entire CNV was visible on the 3 × 3-mm scan area were included to allow consistent measuring of CNV during follow-up with dense OCTA scans. Choroidal neovascularization vessel area was calculated by summing detected flow pixels and represents the total area occupied by individual neovascular vessels. Automatic contouring of the CNV allowed for calculation of CNV membrane area (in square millimeters), a summation of all pixels within the contour. Choroidal neovascularization membrane area is analogous to calculations of CNV area with FA and ICGA.

Cross-sectional composite SD-OCT and color-coded OCTA images were used to classify CNV in accordance with the proposed anatomic classification of Gass.[24] Lesions with a corresponding flow signal above Bruch's membrane and below the RPE were considered type 1, whereas those with flow signal above the RPE in the subretinal space were considered type 2. Lesions with a flow signal connecting the sub-RPE space into the deep capillary plexus of the inner retina were classified as type 3.[25]

Mean change in CNV vessel area and CNV membrane area were considered statistically significant at a level of $P < 0.05$ using the Wilcoxon test. For those visits with 2 high-quality scans (signal strength index [SSI] >50), mean ± standard deviation values of CNV vessel area and CNV membrane area were calculated at each visit. Repeatability was determined using the coefficient of variation. A second grader (J.W.) independently corrected the segmentation manually when needed for the baseline visits and the first visits after treatment, and intergrader reproducibility was determined with a coefficient of variation.

Results

Fourteen eyes from 14 study participants with treatment-naïve neovascular AMD were enrolled. Three eyes were not included in the analysis because of poor image quality that prevented quantitative assessment and 3 study eyes showed a significant portion of CNV outside the 3 × 3-mm^2 scanning area. Of the 8 remaining eyes, the mean age was 70 years (range, 57−80 years). All eyes were treated with bevacizumab. In a total of 92 visits, 2 high-quality scans were available to calculate within-visit repeatability. Coefficient of variation was 7.96% for CNV vessel area and 7.37% for CNV membrane area. The intergrader reproducibility (coefficient of variation) was 9.3% for CNV vessel area and 8.4% for CNV membrane area.

Five participants showed type 1 CNV lesions and 2 participants showed type 2 lesions on OCTA. The type 1 lesions on OCTA corresponded to occult lesions on FA, and the type 2 lesions on OCTA corresponded to classic CNV on FA. Additionally, 1 eye demonstrated abnormal vasculature associated with the deep capillary plexus as seen on OCTA that was consistent with type 3 CNV, and this corresponded to a retinal angiomatous proliferation lesion on FA.

Choroidal neovascularization vessel area and membrane area were calculated at each visit for each eye. Table 1 summarizes baseline characteristics as well as changes to CNV vessel area over time, and Table 2 highlights changes to CNV membrane area over time. Mean CNV vessel area and mean CNV membrane area each were calculated in 7 of 8 eyes. Patient 2 was excluded from this analysis because the presence of SRH obscured baseline CNV vessel area and membrane area measurements. Mean baseline CNV vessel area was 0.39±0.29 mm^2. Mean CNV vessel area decreased to 0.29±0.26 mm^2 (39% reduction) at month 1 and to 0.26±0.26 mm^2 (50% reduction) at month 3 ($P < 0.05$, Wilcoxon test). After month 3, as more eyes were in the PRN phase of treatment, CNV reduction from baseline was 0.29±0.34

Table 2. Choroidal Neovascularization Membrane Area in Response to Pro Re Nata Anti–Vascular Endothelial Growth Factor Treatment

	Choroidal Neovascularization Membrane Area (mm^2)								
Patient No.	*Initial*	*After 1 Month*	*Change from Baseline (%)*	*After 3 Months*	*Change from Baseline (%)*	*After 6 Months*	*Change from Baseline (%)*	*After Approximately 12 Months*	*Change from Baseline (%)*
1	1.00	0.85	−15	0.83	−18	0.80	−20	0.32	−68
2*	1.30	1.72	33	2.57	98	3.00	131	2.04	57
3	2.23	1.83	−18	1.68	−24	1.76	−21	1.32	−41
4*	0.38	0.32	−16	0.25	−36	0.22	−42	0.27	−29
5	1.48	1.26	−15	0.99	−33	0.85	−43	1.75	18
6	1.40	0.75	−47	0.73	−48	0.55	−61	0.72	−49
7	0.40	0.14	−65	0	−100	0.03	−92	0.21	−48
8	0.06	0	−100	0	−100	0	−100	0	−100
Average†	0.99±0.77	0.74±0.65‡	−39±33	0.64±0.61‡	−51±35	0.60±0.62‡	−54±32	0.66±0.65	−45±36

*Indicates participant was treated at every visit.
†Average (mean ± standard deviation) values do not include patient 2.
‡$P < 0.05$ when compared with baseline (Wilcoxon test); does not include patient 2.

mm^2 (43%) and 0.29±0.29 mm^2 (41%) at months 6 and 12, respectively, a difference that was no longer statistically significant (Table 1).

Baseline mean CNV membrane area was 0.99±0.77 mm^2, decreasing to 0.74±0.65 mm^2 (39%), 0.64±0.61 mm^2 (51%), and 0.60±0.62 mm^2 (54%) at months 1, 3, and 6, respectively ($P < 0.05$, Wilcoxon test). At month 12, mean CNV membrane area was 0.66±0.65 mm^2 (45% reduction), a value no longer statistically significant.

Collectively, the general trend was a reduction in CNV vessel area over time while receiving PRN treatment. However, comparing individual changes in CNV vessel area over time revealed that each eye demonstrated a unique response to treatment. Individual patients categorized by number of injections provided are described in Figure 1.

Frequent Treatment Required

Three of 8 eyes (patients 2, 4, and 8) received treatment at nearly every visit during the study. In 2 of these patients (patients 2 and 4), this was because of persistent fluid on OCT meeting re-treatment criteria. Patient 2 showed a type 1 CNV and was the only patient in whom CNV metrics increased in concert with resolution of SRH. Baseline ICGA revealed larger CNV measuring 3.5 mm^2 compared with 1.30-mm^2 CNV membrane area measured with OCTA. This demonstrates that light scatter from SRH was interfering with OCTA-derived CNV vessel area and membrane area measurements (Fig 2). Choroidal neovascularization vessel area and membrane area increased at months 1 and 2 while receiving treatment because of resolution of SRH, which improved OCTA signal. After resolution of SRH at month 2, CNV vessel area subsequently declined with further treatment, which was required because of the presence of fluid on OCT. In patient 4, a type 1 CNV was associated with persistent fluid that required frequent treatment. Over the course of 1 year, CNV vessel area and membrane area fluctuated from visit to visit, and at 1 year, they were 29% and 27% smaller compared with baseline, respectively. One eye (patient 8) showed a type 3 CNV, and after a single treatment, all flow on OCTA and all fluid on SD-OCT had resolved (Fig 3). However, persistent intraretinal hemorrhage was present for 2 months. The patient declined PRN treatment and was treated monthly until month 12. At 12 months, no fluid was present on OCT, no flow was evident on OCTA, and all hemorrhage had resolved.

Treatment of Choroidal Neovascularization Withheld without Reactivation

Two eyes (patients 3 and 6) did not require further treatment after entering the PRN phase of treatment. In patient 3, a type 1 CNV showed a 12% reduction in CNV vessel area after initial treatment. After 2 injections, subsequent treatment was deferred because of failure to meet retreatment criteria, and CNV vessel area fluctuated and gradually increased over time; however, recurrent exudation did not develop. Patient 6 was notable in that during the first 6 months of treatment, cross-sectional OCTA showed envelopment of the vascularized subretinal tissue by a hyperreflective layer contiguous with the surrounding RPE (Fig 4). What initially was characterized as type 2 CNV developed the appearance of a pigment epithelial detachment and type 1 anatomic features. The timing of this occurrence coincided with cessation of detectable disease activity. After extended follow-up of 24 months, no further treatment was required and CNV vessel area and membrane area have remained stable.

Treatment Withheld and Retreatment Subsequently Required

In 3 eyes (patients 1, 5, and 7), treatment was withheld and then restarted when retreatment criteria were met at a later date. In patient 1, type 1 CNV, reduced CNV vessel area, and membrane area were associated with 3 monthly bevacizumab injections, at which time injections were withheld. At month 5 and 6, CNV vessel area increased, whereas there was minimal change in CNV membrane area (Fig 5). During this time, structural OCT showed no recurrence of SRF or IRF and an injection was not administered (Fig 6). Evaluation at month 6 showed a further increase in CNV vessel area as well as the presence of recurrent SRF on OCT. These events suggest that changes seen on OCTA may precede fluid recurrences as seen on structural OCT. In this example, CNV vessel area increased before fluid, whereas there was minimal change in CNV membrane area, suggesting that CNV vessel area may be a more sensitive metric. Two additional bevacizumab injections were administered (at months 6 and 7), and no further signs of disease activity were seen over the study period. Between months 10 and 11, CNV vessel area and CNV membrane area decreased spontaneously without treatment, and this trend was maintained during subsequent visits. During this

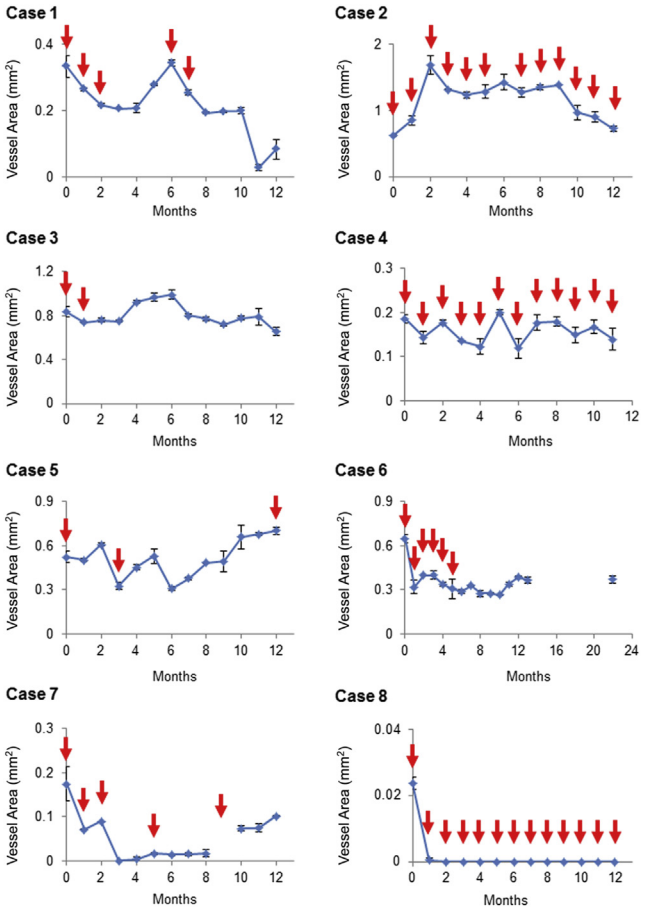

Figure 1. Graphical representations of changes in choroidal neovascularization vessel area over time for patients 1 through 8. *Red arrows* indicate time points at which anti–vascular endothelial growth factor treatment was administered. Error bars indicate standard deviation.

period when spontaneous reduction in flow was detected with OCTA, there were no systemic health changes or changes in medications, and blood pressure remained stable.

In patient 7, who showed a type 2 CNV after 3 monthly injections, all CNV flow became immeasurable with OCTA and all fluid on structural OCT resolved. At months 3 and 4, treatment was not indicated. At month 5, new visual symptoms developed and new subretinal hyperreflective material (SHRM) was seen on structural OCT. Neovascular vessels associated with the SHRM were detected on OCTA, and both CNV vessel area and membrane area began to increase. After 1 injection, symptoms improved and the area of SHRM resolved. With OCTA, CNV flow continued to be detected at months 6, 7, and 8; however, treatment was not indicated based on absence of fluid on structural OCT. At month 9, recurrence of both SRF and SHRM was noted on structural OCT. Treatment was required at month 9, but unfortunately, the study participant did not have time to undergo OCTA on that day. After this visit, CNV vessel area and membrane area continued to increase slightly in subsequent visits without the need for re-treatment.

Patient 5 illustrates a situation in which treatment with anti-VEGF did not seem to affect type 1 CNV. Minimal change was noted in this type 1 CNV after initial treatment. At month 3, the CNV vessel area and membrane area decreased; however, treatment was administered because of a small amount of IRF present on structural OCT. After this treatment, CNV vessel area seemed to increase in subsequent visits. Then, after a spontaneous reduction in CNV flow metrics at month 5, flow gradually increased over the next 6 visits, with treatment needed at the final visit of the study. In this case, anti-VEGF treatment may have had more effect on vascular permeability and less effect on the CNV flow that was detected by OCTA.

Discussion

This is the first prospective case series we are aware of that used OCTA to monitor quantitative flow changes in treatment-naïve CNV during 1 year of anti-VEGF treatment under a PRN protocol. At the months 1 and 3 follow-up visits, most eyes showed reductions in both CNV vessel area and membrane area in response to anti-VEGF treatment, and the mean vessel and membrane areas were reduced significantly. At each of these time points, the magnitude of the reduction of both CNV vessel area and membrane area were greater than the calculated within-visit coefficients of variation, suggesting that measured reductions in CNV flow are real and are not related solely to variations in scan quality. Although several other studies have used OCTA to demonstrate reductions in CNV flow in treatment-naïve eyes, these studies had variable follow-up intervals and did not follow a prespecified treatment protocol.[15,16,18,20,26] Prior studies using FA-based measurements found that CNV size remained stable after 1 year of monthly anti-VEGF treatment[27] and that CNV size increased slightly when switched to a PRN treatment protocol.[7] In our study, CNV membrane area and vessel area were reduced at 1 year in most eyes, and the mean reductions were 45% and 41%, respectively. It is not surprising that FA and OCTA results do not correlate well because CNV size measurements with FA are dependent on leakage and staining patterns that may be influenced by the morphologic features of surrounding tissues, such as fibrosis or detachment of the pigment epithelium. In contrast, OCTA detects moving red blood cells to calculate quantitative flow metrics, and changes in blood flow may be more sensitive to anti-VEGF treatment. The presence of CNV exudation on structural OCT (as indicated by intraretinal or subretinal fluid) commonly is used as a surrogate for CNV activity and guides administration of anti-VEGF therapy.

It previously was shown that CNV surface area measurements with ICGA can be predictive of exudation on OCT.[28] In the current series, OCTA showed each patient to have a unique response (Fig 1) to anti-VEGF treatment, and increases in CNV vessel area and membrane area did not always correlate with presence of exudation. A comparison of patients 1 and 5, both with type 1 CNV, provides an example. In patient 1, a relatively rapid increase in CNV vessel area of 25% between months 4 and 5 followed by an increase of 18% between months 5 and 6 preceded the recurrence of SRF, and the need for treatment suggested that increased vessel area may be associated with exudation. In patient 5, between months 2 and 3, CNV vessel area decreased spontaneously by 46% without anti-VEGF treatment. Then, despite further reduction in vessel area at month 4, a small amount of IRF developed and treatment was

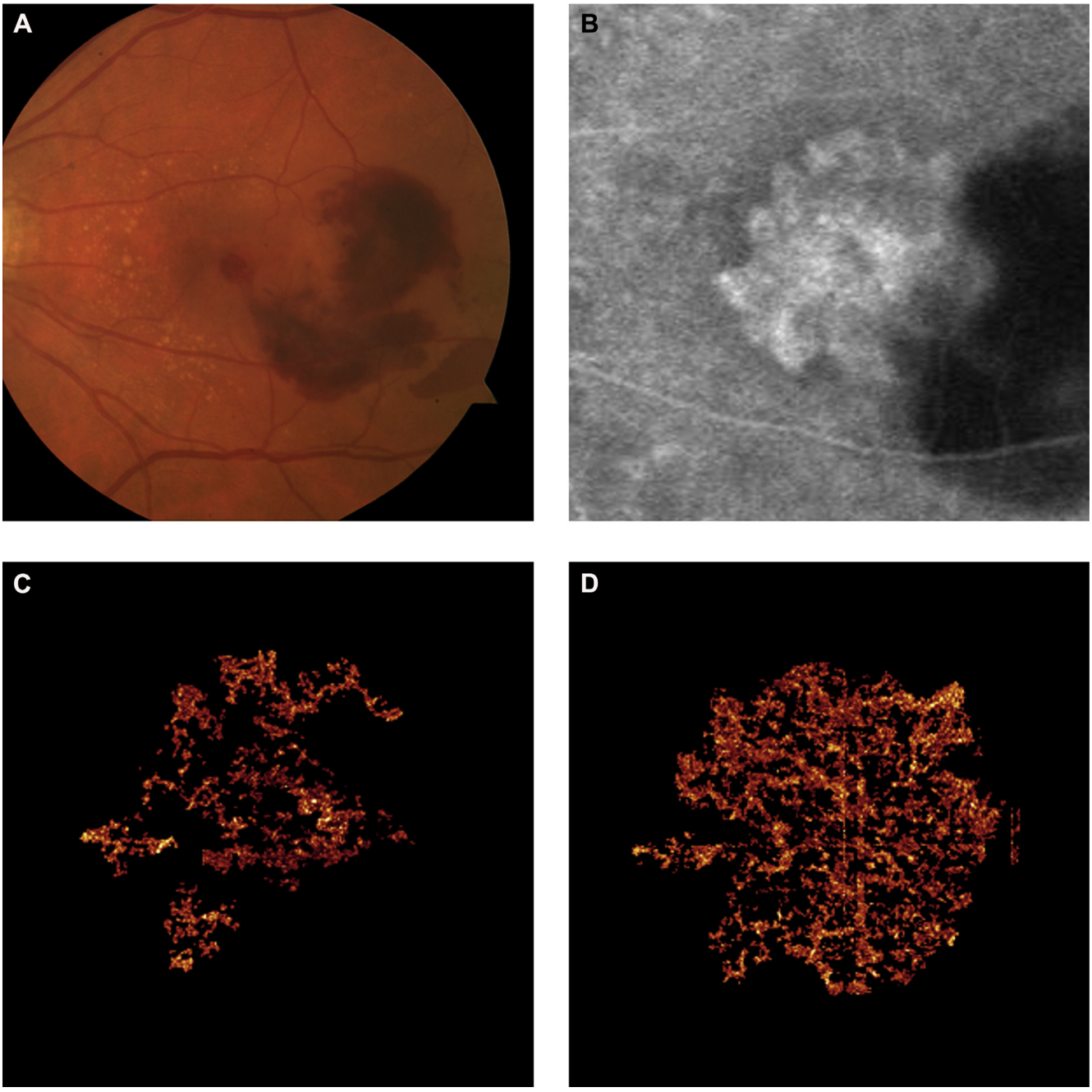

Figure 2. Images from patient 2. **A**, Color fundus photograph obtained at baseline showing drusen, pigmentary changes, and subretinal hemorrhage (SRH). **B**, Late-phase indocyanine green angiogram obtained at baseline showing hyperfluorescent plaque consistent with a choroidal neovascularization (CNV) membrane. There is partial obscuration of the temporal border of the membrane because of blockage resulting from SRH. **C**, Baseline outer retinal OCT angiography (OCTA) image revealing CNV. However, SRH obstructs portions of the OCTA signal. **D**, Outer retinal OCTA obtained at month 3 after consecutive monthly anti–vascular endothelial growth factor treatments. Choroidal neovascularization becomes more visible as SRH resolves and has similar appearance as baseline indocyanine green angiogram.

recommended. After treatment, CNV vessel area fluctuated and increased gradually; however, treatment was not indicated until month 12. Comparing these 2 patients highlights that changes in OCTA-derived CNV vessel area may be predictive of exudation in some, but not all, cases of CNV. Because anti-VEGF affects both angiogenesis and vascular permeability, it is possible that for some patients with CNV, such as patient 5, anti-VEGF treatment is more effective in reducing vascular permeability than in reducing CNV blood flow. In other patients, anti-VEGF may have a greater effect on inhibiting angiogenesis and thereby reducing flow within the CNV, such as in patient 1.

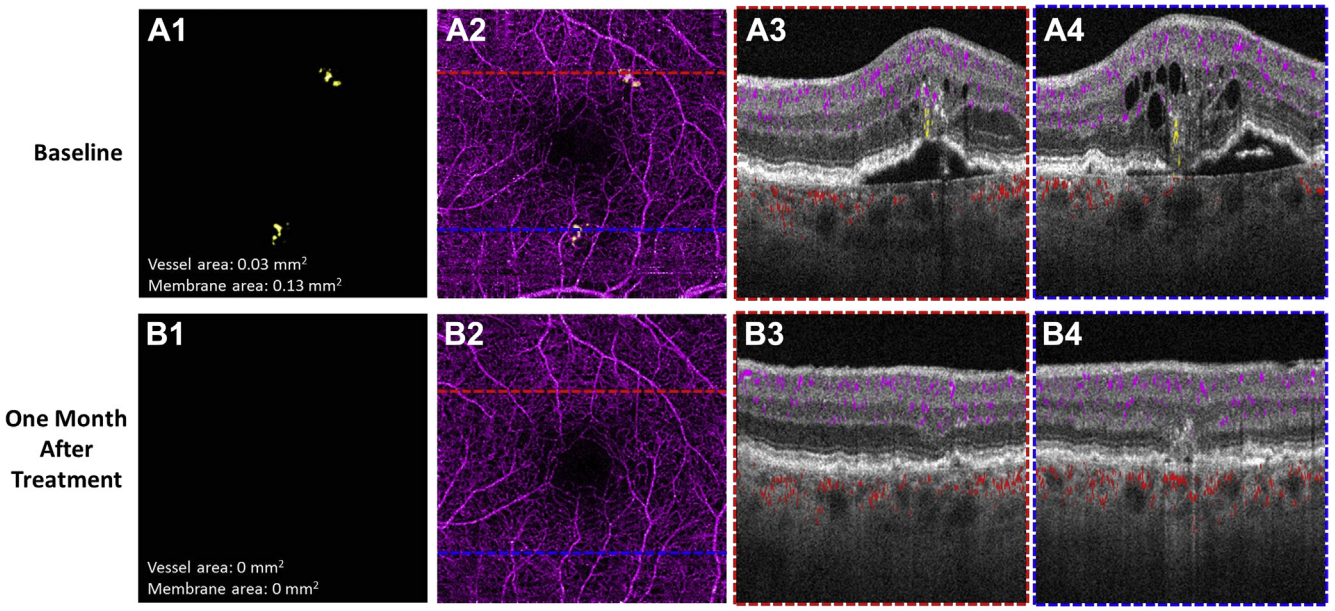

Figure 3. Images from patient 8. **A1**–**A4**, Baseline OCT angiography (OCTA) images showing type 3 choroidal neovascularization (CNV). **A1**, En face outer retinal slab showing type 3 lesions. **A2**, Inner retinal slab with retinal vessels in purple and type 3 CNV highlighted with *pink*. Cross-sectional OCTA showing blood flow (*yellow*) of (**A3**) superior type 3 CNV (corresponds to *red line* in **A2**) and of (**A4**) inferior type 3 CNV (corresponds to *red line* in **A2**). **B1**–**B4**, One month after bevacizumab treatment. Resolution of type 3 CNV in (**B1**) outer retinal slab and (**B2**) inner retinal slab. Cross-sectional OCTA image showing loss of detected blood flow and resolution of pigment epithelial (RPE) detachment.

Prior work has demonstrated that multimodal imaging can be used to classify CNV as type 1, 2, or 3 and that this classification may be clinically meaningful in the anti-VEGF era.[25] OCT angiography has the advantage of being able to classify lesion type by detecting depth of flow in relation to RPE on cross-sectional OCTA, and this information can be used to compare treatment response directly between CNV types. In this study, 1 month after the first treatment, type 1 CNV showed a CNV vessel area reduction ranging from 4% to 23%, whereas the 2 patients with type 2 CNV showed larger-magnitude reductions of 51% and 60%. The small number of type 2 eyes in this series limits any firm conclusions that type 2 eyes are more responsive to anti-VEGF treatment; however, these findings agree with those reported by Coscas et al,[18] who used OCTA to show that type 2 CNV had a greater reduction with treatment compared with type 1 CNV. Furthermore, our results for type 1 treatment response were similar to

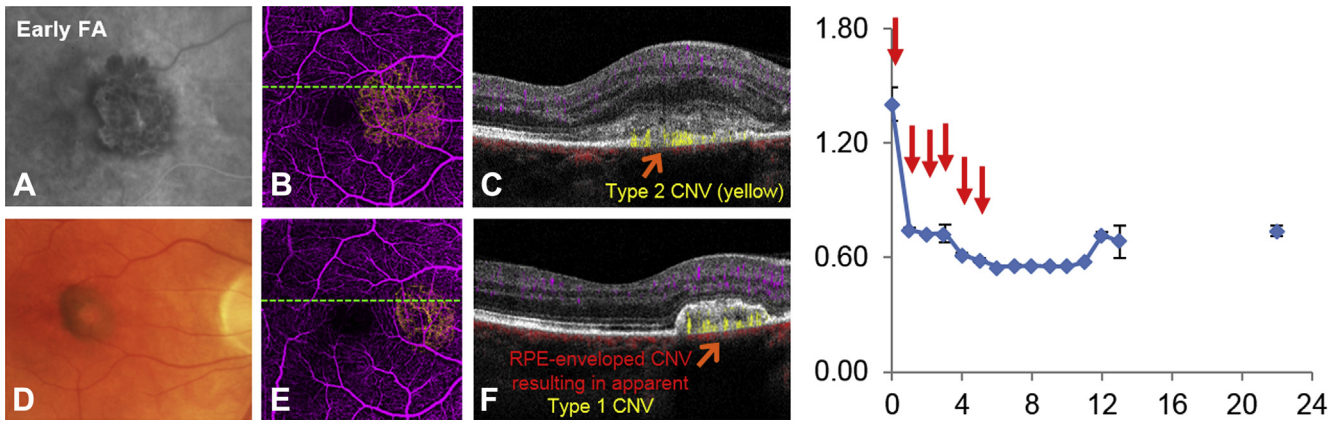

Figure 4. Images from patient 6: (**A**–**C**) at baseline and (**D**–**F**) after 6 monthly injections. **A**, Early fluorescein angiography (FA) obtained at baseline showing a choroidal neovascularization (CNV) membrane. **B**, OCT angiography (OCTA) image obtained at baseline showing flow in outer retinal space consistent with CNV (*yellow*). **C**, Cross-sectional composite OCT image obtained at baseline (corresponds to location of *green dashed line* in **B**) showing type 2 configuration of CNV. **D**, Color fundus photograph obtained at 6 months showing pigmented subretinal lesion. **E**, OCT angiography image obtained at 6 months showing reduced CNV flow (*yellow*). **F**, Cross-sectional composite OCT image obtained at 6 months (corresponds to location of *green dashed line* in **E**) showing retinal pigment epithelium (RPE) envelopment of the CNV, which now has a type 1 appearance. Composite OCT and OCTA legend: *purple*, inner retinal flow signal; *yellow*, outer retinal flow signal; *red*, choroidal flow signal.

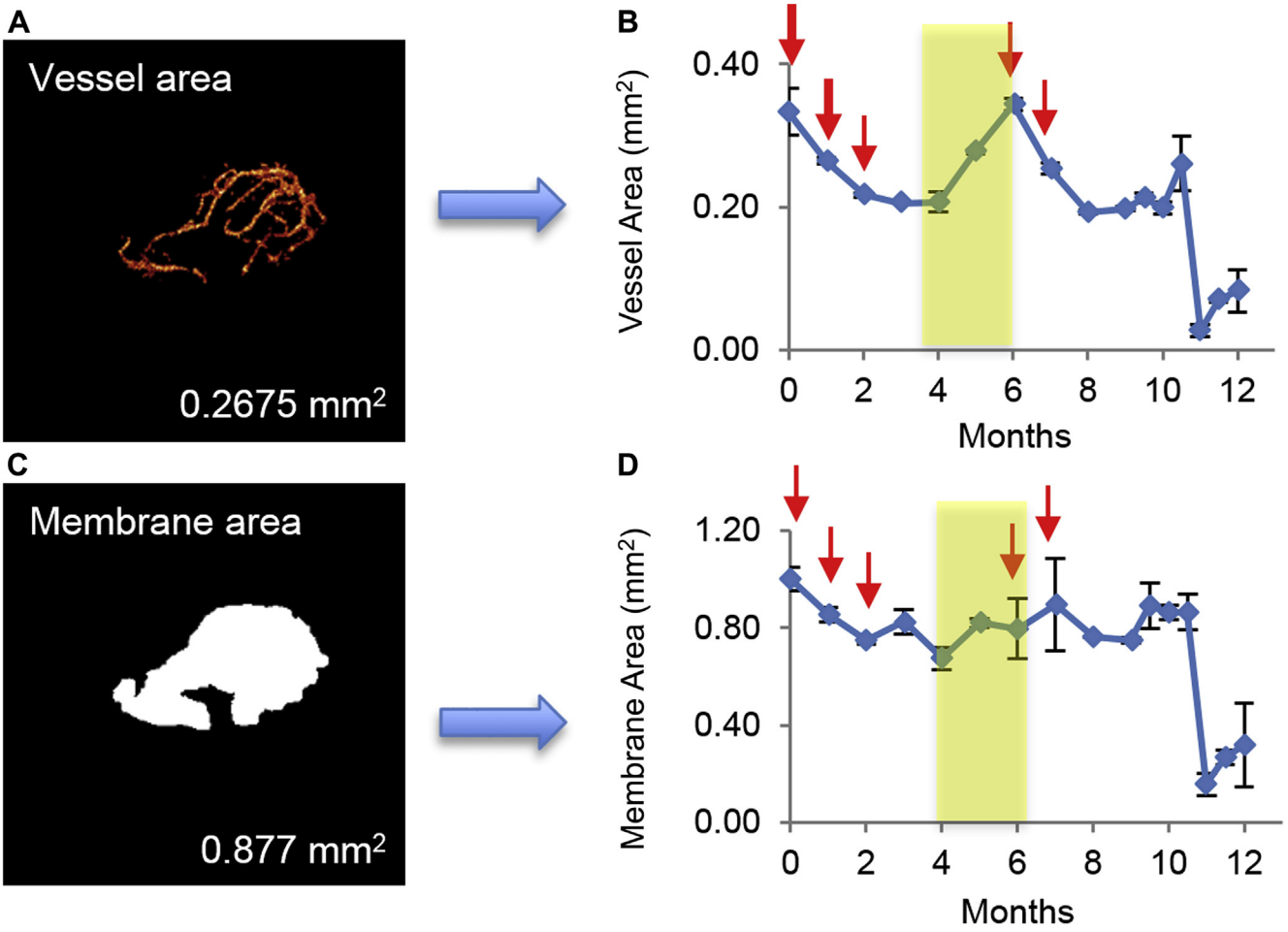

Figure 5. Images from patient 1. Outer retinal OCT angiography images obtained after removal of projection artifact showing the flow metrics of (**A**) choroidal neovascularization (CNV) vessel area and (**B**) CNV membrane area. **C** and **D**, Graphical representations of changes in CNV vessel area (**B**) and CNV membrane area (**D**) over time for patient 1. *Red arrows* indicate time points where anti–vascular endothelial growth factor treatment was administered. At month 6, re-treatment criteria were met, and the in the preceding visits (*yellow shaded area*), CNV vessel area increased to baseline value, whereas CNV membrane area remained stable, suggesting that CNV vessel area and membrane area may not always coincide with one another. Error bars indicate standard deviation.

those reported by Querques et al,[29] who found reduced CNV surface area with ICGA at 1 year while receiving PRN anti-VEGF treatment; however, this was not statistically significant compared with baseline. In our study, the lone type 3 CNV patient (patient 8) showed complete resolution of IRF on structural OCT and flow on OCTA after a single treatment. The type 3 CNV was small, and the robust treatment response may have been the result of the relatively early initiation of anti-VEGF.[30–32] In this patient, ongoing treatment was given because the intraretinal hemorrhage persisted for several months, and then it was continued because of the patient's preference. Larger studies are needed to validate if the different CNV subtypes based on OCTA can be predictive of unique treatment response with anti-VEGF therapy. Finally, patient 6 (Fig 3) is an example of a RPE cells enveloping a type 2 CNV resulting in an apparent type 1 CNV, an event Gass[33] postulated based on histologic features. Identifying this phenotype with structural OCT along with stable CNV vessel area over time with OCTA may help clinicians to identify CNVs that are at low risk for exudation developing without anti-VEGF treatment.

With OCTA, multiple different metrics are available for CNV for quantification. In this study, we used vessel area and membrane area. Both CNV vessel area and membrane area had a similar within-visit repeatability and intergrader reproducibility. In most of the patients presented herein, each metric yielded similar results. Choroidal neovascularization vessel area was reduced by 39%, 50%, 43%, and 41% at months 1, 3, 6, and 12, respectively. Choroidal neovascularization membrane area was reduced by 39%, 51%, 54%, and 45% at months 1, 3, 6, and 12, respectively. At month 6, mean change from baseline was not statistically significant for CNV vessel area, whereas it was statistically significant for CNV membrane area. This suggests that these parameters are not entirely interchangeable. An example of

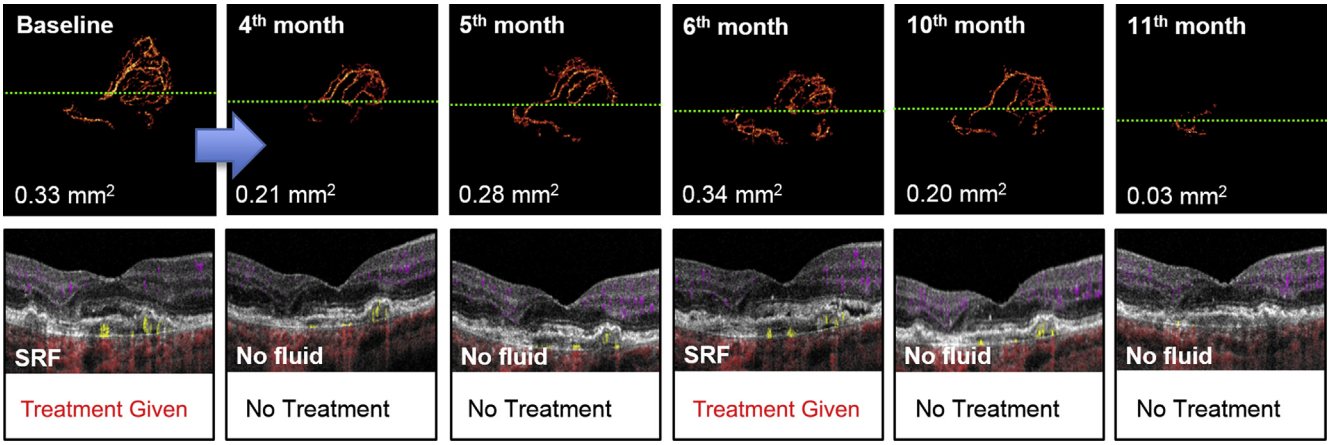

Figure 6. Images from patient 1. Outer retinal OCT angiography (OCTA) images and corresponding cross-sectional composite OCT images obtained at baseline and during follow-up under pro re nata anti–vascular endothelial growth factor treatment. Monthly injections were given over the first 3 visits (*blue arrow*). Choroidal neovascularization (CNV) vessel area decreased over the first 3 injections, and no treatment was indicated at month 4 because of resolution of subretinal fluid (SRF). Choroidal neovascularization vessel area increased during month 5; however, no fluid was present and treatment was not provided. At month 6, choroidal neovascularization CNV vessel area continued to enlarge to baseline level, and SRF recurred while treatment was withheld, demonstrating that OCTA can detect increasing CNV vessel area in the absence of exudation. There is dramatic spontaneous reduction in CNV size without treatment between months 10 and 11. *Green dashed lines* correspond to locations of composite OCT images at each time point. Composite OCT legend: *purple*, inner retinal flow signal; *yellow*, outer retinal flow signal; *red*, choroidal flow signal.

the difference of vessel area and membrane area is highlighted in patient 1. During the 4 to 6 months that preceded the development of SRF while treatment was withheld, CNV vessel area increased sharply, whereas CNV membrane area remained relatively stable (Fig 5). Membrane area reflects the overall footprint of the membrane and does not account for changes within the footprint. Vessel area can detect vascular changes better within the footprint, such as branches enlarging or shrinking or changes in the caliber of vessels. This suggests that CNV vessel area may correlate better with CNV activity compared with membrane area. Because it is easy to apply multiple quantitative analyses to the same scan, larger studies will be able to compare the usefulness of different quantitative metrics.

Meaningful quantitative metrics derived from OCTA require high-quality scans and steps to address segmentation errors and projection artifacts. At each visit, 2 scans were obtained. Ninety-two visits had 2 high-quality scans, and averaged CNV vessel area and membrane were used. If only 1 high-quality scan was available (i.e., there were excessive motion artifacts in one scan but not both), only the higher-quality scan was used for analysis. Coefficient of variation calculation showed good within-visit repeatability for both CNV vessel area and membrane. For each scan at each visit, segmentation was reviewed throughout the entire volume, and manual segmentation was used to correct errors. Manual segmentation correction is a time-consuming process, but it is imperative for ensuring accuracy because quantitative metrics are derived from en face images and inaccurate segmentation will lead to misleading metrics. However, the process of manual segmentation itself introduces variability evidenced by the intergrader reproducibility of 9.3% for CNV vessel area and 8.4% for CNV membrane area. Projection artifact was addressed using a slab subtraction technique that mitigates, but does not eliminate, projection artifact. Other groups also demonstrated the slab subtraction method to be effective for CNV detection.[28] Newer projection artifact removal techniques have been shown to reduce artifact without attenuating the CNV signal, and these will be tested in future studies.[34] Finally, an automated, saliency-based detection method was used that has been shown to be less variable than manual contouring.[22]

There are several aspects of this study that limit generalizations that can be made to real-world clinical practice. The most notable limitation is the small sample size of this study. For example, at 1 year, CNV vessel area and membrane area were reduced by more than 40%; however, this was not statistically significant because of limited statistical power. Retinal vessel density values have been shown to correlate with SSI, and although all scans included in the analysis had an SSI of more than 50, that does not exclude the possibility of that variation in SSI at different visits may have affected CNV vessel density measurements.[35,36] Also, because scans were obtained monthly, potential variations in the metrics between visits remain unknown. Lumbroso et al[37] noted dramatic reductions in CNV vessel area measurements within the first 10 days after treatment with subsequent reperfusion of CNV later on. These changes would have been missed in the present study; however, their clinical relevance also is unclear. Finally, although the extensive processing after imaging is helpful to achieve meaningful quantitative data, it is time consuming and unrealistic for this to be achieved in a busy clinical practice. As OCTA technology and automated image processing improves, reliable quantitative metrics should become available on commercial machines.

The study also has its strengths. It was designed prospectively, and quantitative changes in CNV flow patterns

were tracked over time while under a strict protocol of PRN anti-VEGF treatment. The sole exception to this occurred in patient 8, who decided in the middle of the study to forego the PRN protocol in favor of monthly treatment. Study coordinators also were used to contact patients to arrange for consistent intervals between visits and treatments. Great care was taken to ensure that quantitative OCTA metrics were as accurate as possible by applying manual segmentation correction, reducing the impact of artifacts, and evaluating the within-visit repeatability to reduce the chance that observed changes were the result of expected scan-to-scan variation. Finally, this is the first report comparing the quantitative metrics of CNV vessel area with CNV membrane area, showing agreement in most, but not all, visits (Fig 4). This study suggests that CNV vessel area may be a more sensitive metric for detecting changes CNV blood flow compared with CNV membrane area.

Conclusions

This small case series used OCTA to demonstrate a reduction in CNV vessel area and membrane area in response to the first 3 months of PRN anti-VEGF treatment. After 1 year of PRN treatment, CNV vessel area and membrane area were reduced; however, these changes were not statistically significant compared with baseline. Longitudinal follow-up revealed that each CNV showed a unique response to anti-VEGF treatment as well as variable changes in CNV vessel area when anti-VEGF treatment was deferred. Increasing CNV vessel area tended to correlate with future exudation, but was less useful in predicting exactly when exudation develops. Future studies comparing fixed monthly treatment with a PRN or treat-and-extend protocol would be useful to evaluate better how anti-VEGF treatment affects blood flow in CNV measured with OCTA and whether OCTA can be useful in predicting when exudation will develop.

References

1. Ambati J, Ambati BK, Yoo SH, et al. Age-related macular degeneration: etiology, pathogenesis, and therapeutic strategies. *Surv Ophthalmol*. 2003;48:257–293.
2. Mokwa NF, Keane PA, Kirchhof B, et al. Grading of age-related macular degeneration: comparison between color fundus photography, fluorescein angiography, and spectral domain optical coherence tomography. *J Ophthalmol*. 2013;2013:1–6.
3. Rosenfeld PJ. Optical coherence tomography and the development of antiangiogenic therapies in neovascular age-related macular degeneration. *Invest Ophthalmol Vis Sci*. 2016;57:OCT14–OCT26.
4. Brown DM, Kaiser PK, Michels M, et al. Ranibizumab versus verteporfin for neovascular age-related macular degeneration. *N Engl J Med*. 2006;355:1432–1444.
5. Schmidt-Erfurth U, Eldem B, Guymer R, et al. Efficacy and safety of monthly versus quarterly ranibizumab treatment in neovascular age-related macular degeneration: the EXCITE study. *Ophthalmology*. 2011;118:831–839.
6. Abraham P, Yue H, Wilson L. Randomized, double-masked, sham-controlled trial of ranibizumab for neovascular age-related macular degeneration: PIER study year 2. *Am J Ophthalmol*. 2010;150:315–324.e1.
7. CATT Research Group, Martin DF, Maguire MG, et al. Ranibizumab and bevacizumab for neovascular age-related macular degeneration. *N Engl J Med*. 2011;364:1897–1908.
8. Wykoff CC, Croft DE, Brown DM, et al. Prospective Trial of Treat-and-Extend versus Monthly Dosing for Neovascular Age-Related Macular Degeneration: TREX-AMD 1-year results. *Ophthalmology*. 2015;122:2514–2522.
9. Rush RB, Rush SW, Aragon AV, Ysasaga JE. Predictability of recurrent exudation and subretinal hemorrhaging in neovascular age-related macular degeneration with indocyanine green angiography. *Ophthalmic Surg Lasers Imaging Retina*. 2015;46:718–723.
10. Jia Y, Tan O, Tokayer J, et al. Split-spectrum amplitude-decorrelation angiography with optical coherence tomography. *Opt Express*. 2012;20:4710–4725.
11. Motaghiannezam R, Fraser S. Logarithmic intensity and speckle-based motion contrast methods for human retinal vasculature visualization using swept source optical coherence tomography. *Biomed Opt Express*. 2012;3:503–521.
12. Jia Y, Bailey ST, Hwang TS, et al. Quantitative optical coherence tomography angiography of vascular abnormalities in the living human eye. *Proc Natl Acad Sci U S A*. 2015;112:E2395–E2402.
13. Jia Y, Bailey ST, Wilson DJ, et al. Quantitative optical coherence tomography angiography of choroidal neovascularization in age-related macular degeneration. *Ophthalmology*. 2014;121:1435–1444.
14. Moult E, Choi W, Waheed NK, et al. Ultrahigh-speed swept-source OCT angiography in exudative AMD. *Ophthalmic Surg Lasers Imaging Retina*. 2014;45:496–505.
15. Kuehlewein L, Bansal M, Lenis TL, et al. Optical coherence tomography angiography of type 1 neovascularization in age-related macular degeneration. *Am J Ophthalmol*. 2015;160:739–748.e2.
16. De Carlo TE, Bonini F, Waheed NK, et al. Spectral-domain optical coherence tomography angiography of choroidal neovascularization. *Ophthalmology*. 2015;122:1–11.
17. Coscas GJ, Lupidi M, Coscas F, et al. Optical coherence tomography angiography versus traditional multimodal imaging in assessing the activity of exudative age-related macular degeneration: a new diagnostic challenge. *Retina*. 2015;35:2219–2228.
18. Coscas G, Lupidi M, Coscas F, et al. Optical coherence tomography angiography during follow-up: qualitative and quantitative analysis of mixed type I and II choroidal neovascularization after vascular endothelial growth factor trap therapy. *Ophthalmic Res*. 2015;54:57–63.
19. Spaide RF. Optical coherence tomography angiography signs of vascular abnormalization with antiangiogenic therapy for choroidal neovascularization. *Am J Ophthalmol*. 2015;160:6–16.
20. Kuehlewein L, Sadda SR, Sarraf D. OCT angiography and sequential quantitative analysis of type 2 neovascularization after ranibizumab therapy. *Eye (Lond)*. 2015;29:932–935.
21. Liang MC, De Carlo TE, Baumal CR, et al. Correlation of spectral domain optical coherence tomography angiography and clinical activity in neovascular age-related macular degeneration. *Retina*. 2016;36:2265–2273.
22. Liu L, Gao SS, Bailey ST, et al. Automated choroidal neovascularization detection algorithm for optical coherence tomography angiography. *Biomed Opt Express*. 2015;6:3564–3576.
23. Zhang M, Wang J, Pechauer AD, et al. Advanced image processing for optical coherence tomographic angiography of macular diseases. *Biomed Opt Express*. 2015;6:4661–4675.

24. Gass JDM. *Stereoscopic Atlas of Macular Diseases*. Nashville, TN: Mosby Incorporated; 1996.
25. Freund KB, Zweifel SA, Engelbert M. Do we need a new classification for choroidal neovascularization in age-related macular degeneration? *Retina*. 2010;30:1333−1349.
26. Muakkassa NW, Chin AT, de Carlo T, et al. Characterizing the effect of anti-vascular endothelial growth factor therapy on treatment-naive choroidal neovascularization using optical coherence tomography angiography. *Retina*. 2015;35:2252−2259.
27. Kaiser PK, Blodi BA, Shapiro H, Acharya NR. Angiographic and optical coherence tomographic results of the MARINA study of ranibizumab in neovascular age-related macular degeneration. *Ophthalmology*. 2007;114:1868−1875.e4.
28. Rush RB, Rush SW. Predictability of recalcitrance in neovascular age-related macular degeneration with indocyanine green angiography. *Asia Pac J Ophthalmol*. 2015;4:187−190.
29. Querques G, Tran THC, Forte R, et al. Anatomic response of occult choroidal neovascularization to intravitreal ranibizumab: a study by indocyanine green angiography. *Graefes Arch Clin Exp Ophthalmol*. 2012;250:479−484.
30. Tan ACS, Dansingani KK, Yannuzzi LA, et al. Type 3 neovascularization imaged with cross-sectional and en face optical coherence tomography angiography. *Retina*. 2017;37:234−246.
31. Yannuzzi LA, Freund KB, Takahashi BS. Review of retinal angiomatous proliferation or type 3 neovascularization. *Retina*. 2008;28:375−384.
32. Miere A, Querques G, Semoun O, et al. Optical coherence tomography angiography changes in early type 3 neovascularization after anti-vascular endothelial growth factor treatment. *Retina*. 2015;35:2236−2241.
33. Gass JD. Biomicroscopic and histopathologic considerations regarding the feasibility of surgical excision of subfoveal neovascular membranes. *Trans Am Ophthalmol Soc*. 1994;92:91−111. discussion 111−116.
34. Zhang M, Hwang TS, Campbell JP, et al. Projection-resolved optical coherence tomographic angiography. *Biomed Opt Express*. 2016;7:816−828.
35. Gao SS, Jia Y, Liu L, et al. Compensation for reflectance variation in vessel density quantification by optical coherence tomography angiography. *Investig Opthalmology Vis Sci*. 2016;57:4485−4492.
36. Rao HL, Pradhan ZS, Weinreb RN, et al. Determinants of peripapillary and macular vessel densities measured by optical coherence tomography angiography in normal eyes. *J Glaucoma*. 2017;26:491−497.
37. Lumbroso B, Rispoli M, Savastano MC, et al. Optical coherence tomography angiography study of choroidal neovascularization early response after treatment. *Dev Ophthalmol*. 2016;56:77−85.

Footnotes and Financial Disclosures

Originally received: August 5, 2017.
Final revision: January 3, 2018.
Accepted: January 23, 2018.
Available online: ■■■. Manuscript no. ORET_2017_298.

Casey Eye Institute, Oregon Health & Science University, Portland, Oregon.

Financial Disclosure(s):
The author(s) have made the following disclosure(s): Simon Gao: Employee - Genentech

Andreas K. Lauer: Financial support − Genentech, Oxford BioMedica, Allergan, Clearside Biomedical

David Huang: Financial support, Equity owner, Patent royalties, Research equipment − Optovue, Inc.

Yali Jia: Patent royalties − Optovue, Inc.

Steven T. Bailey: Research equipment − Optovue, Inc.

Supported by the National Institutes of Health, Bethesda, Maryland (grant nos.: R01 EY024544, R01EY027833, DP3 DK104397, and P30 EY010572); the Champalimaud Foundation, Lisbon, Portugal (D.H.); and Research to Prevent Blindness, Inc., New York, New York.

HUMAN SUBJECTS: Human subjects were included in this study. The institutional review board of Oregon Health and Science University approved the study, and informed consent to participate in the study was obtained from all patients.

Author Contributions:

Conception and design: Jia, Bailey

Analysis and interpretation: McClintic, Gao, Wang, Hagag, Huang, Jia, Bailey

Data collection: McClintic, Gao, Wang, Hagag, Flaxel, Bhavsar, Hwang, Huang, Jia, Bailey, Lauer

Overall responsibility: McClintic, Gao, Huang, Jia, Bailey

Abbreviations and Acronyms:
AMD = age-related macular degeneration; **CNV** = choroidal neovascularization; **FA** = fluorescein angiography; **ICGA** = indocyanine green angiography; **IRF** = intraretinal fluid; **OCT** = optical coherence tomography; **OCTA** = OCT angiography; **PRN** = pro re nata; **RPE** = retinal pigment epithelium; **SD** = spectral-domain; **SHRM** = subretinal hyperreflective material; **SRF** = subretinal fluid; **SRH** = subretinal hemorrhage; **SSI** = signal strength index; **VEGF** = vascular endothelial growth factor.

Correspondence:
Steven T. Bailey, MD, Casey Eye Institute, Oregon Health & Science University, 3375 SW Terwilliger Boulevard, Portland, OR 97239. E-mail: bailstev@ohsu.edu.